Geophysical Research Letters

RESEARCH LETTER
10.1029/2021GL092520

Special Section:
Fire in the Earth System

Compound Extremes Drive the Western Oregon Wildfires of September 2020

John T. Abatzoglou[1], David E. Rupp[2], Larry W. O'Neill[2,4], and Mojtaba Sadegh[3]

[1]Management of Complex Systems Department, University of California, Merced, CA, USA, [2]Oregon Climate Change Research Institute, College of Earth, Ocean, and Atmospheric Sciences, Oregon State University, Corvallis, OR, USA, [3]Department of Civil Engineering, Boise State University, Boise, ID, USA, [4]Oregon Climate Service, College of Earth, Ocean, and Atmospheric Sciences, Oregon State University, Corvallis, OR, USA

Key Points:

- Approximately 11% of the Oregon Cascades burned during September 7–9, 2020 coincident with strong offshore downslope winds
- Unprecedented compound extremes involving fuel aridity and fire meteorology facilitated the extent and spread of fires
- Very large fires in western Oregon since 1900 have generally occurred during east wind events at the end of anomalously warm-dry summers

Supporting Information:

Supporting Information may be found in the online version of this article.

Correspondence to:

J. T. Abatzoglou,
jabatzoglou@ucmerced.edu

Citation:

Abatzoglou, J. T., Rupp, D. E., O'Neill, L. W., & Sadegh, M. (2021). Compound extremes drive the western Oregon wildfires of September 2020. *Geophysical Research Letters*, *48*, e2021GL092520. https://doi.org/10.1029/2021GL092520

Received 15 JAN 2021
Accepted 8 MAR 2021

Abstract Several very large high-impact fires burned nearly 4,000 km^2 of mesic forests in western Oregon during September 7–9, 2020. While infrequent, very large high-severity fires have occurred historically in western Oregon, the extreme nature of this event warrants analyses of climate and meteorological drivers. A strong blocking pattern led to an intrusion of dry air and strong downslope east winds in the Oregon Cascades following a warm-dry 60-day period that promoted widespread fuel flammability. Viewed independently, both the downslope east winds and fuel dryness were extreme, but not unprecedented. However, the concurrence of these drivers resulted in compound extremes and impacts unmatched in the observational record. We additionally find that most large wildfires in western Oregon since 1900 have similarly coincided with warm-dry summers during at least moderate east wind events. These results reinforce the importance of incorporating a multivariate lens for compound extremes in assessing wildfire hazard risk.

Plain Language Summary Several very large fires in western Oregon spread rapidly during an unusually strong offshore wind event that commenced on Labor Day in 2020. The Labor Day fires burned more area of the Oregon Cascades than had burned in the previous 36 years combined and very likely exceeded the area burned in any single year for at least the past 120 years. The fires damaged over 4,000 structures, led to several fatalities, placed over 10% of the state's residents under some level of evacuation advisory, and contributed to the hazardous air quality across the Northwestern United States. A compound set of weather-related factors leading up to and during the fires facilitated these extreme fires. Unusually warm conditions with limited precipitation in the 60-days leading up to the fires allowed for fuels to become particularly dry and combustible by early September. Downslope offshore winds materialized during September 7–9, 2020 across the Oregon Cascades bringing exceptionally strong winds and dry air that drove rapid rates of fire spread. While neither of these individual factors was unprecedented, the concurrence of these drivers created conditions unmatched in the observational record.

1. Introduction

On Labor Day, September 7, 2020, exceptionally strong east-to-northeast winds developed from Washington state progressing southward in the following days driving extreme fire activity in Washington, Oregon, and California. In western Oregon, the winds fanned several existing small, smoldering wildfires ignited by lightning several weeks prior, and contributed to numerous new human-caused fires that spread rapidly. Dry katabatic winds drove fire spread toward populated areas in the ensuing three days, hindering fire suppression efforts already strained by the numerous concurrent large fires burning across much of the western United States during a fire season of record high atmospheric aridity in much of the region (Higuera & Abatzoglou, 2020). About 40,000 people in Oregon were forced to evacuate their homes, and roughly 500,000 were under some level of evacuation alert during the event. In total, 393,315 hectares burned across 20 fires, all but a few in the Cascades of western Oregon (Figure 1; supporting information). Moreover, over 11% of the Oregon Cascades ecoregion burned in 2020, exceeding the cumulative burned area in the previous 36 years (Figure 1; supporting information) and very likely exceeding annual burned area in western Oregon since at least 1900. The direct cost of the series of fires was estimated at $1.15B USD, which includes the destruction of over 4,000 homes (State of Oregon, 2021).

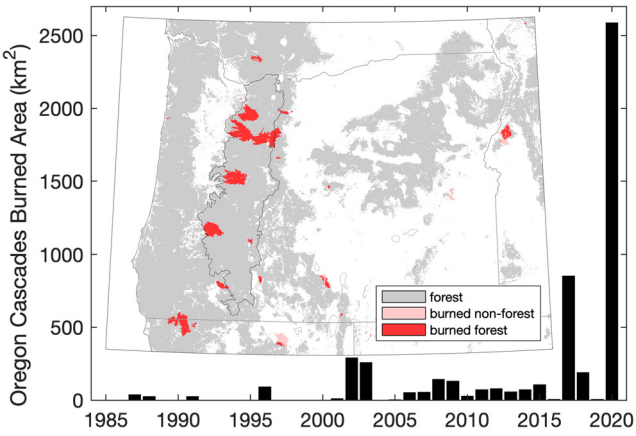

Figure 1. Time series of annual burned area for the portion of the Cascades ecoregion in the State of Oregon for 1984–2020 (black polygon in inset map). Inset map shows perimeters of fires in 2020, including much of the forested burned area in western Oregon that burned during the 7–9 September period.

Sustained strong winds are a major contributor to rapid rates of fire spread, particularly in the presence of dry fuels (Rothermel, 1972). Of particular concern are downslope mountain winds that induce adiabatic warming and entrainment of drier air leeward of mountain barriers. Such winds are a well-recognized critical fire weather pattern in various parts of the globe (Nauslar et al., 2018; Sharples et al., 2010). Offshore downslope winds are a catalyst for large autumn wildfires in California due to the co-occurrence of offshore winds that increase throughout the autumn with dry fuels prior to the arrival of winter precipitation (Guzman-Morales et al., 2016; Kolden & Abatzoglou, 2018). While downslope offshore wind events west of the Cascade Range in the Pacific Northwest are less frequent than counterparts in California (Abatzoglou et al., 2020), significant east wind events have been implicated in major historic fires in western Oregon and Washington (Beals, 1914; Cramer, 1957; Dague, 1930). The earlier arrival of cool-season precipitation and higher fuel moisture in forests along the western flank of the Oregon Cascades compared to California in late summer limit the co-occurrence of extreme fire weather conditions with critically dry fuels.

Traditional univariate hazard assessment approaches for evaluating extreme events such as fire conditioned by interacting drivers, may be ill-posed (Seneviratne et al., 2012); rather, multivariate approaches that incorporate the geographic synchrony, concurrence, and succession of extremes are needed to adequately characterize hazards (Sadegh et al., 2018). Compound drivers have been long implicated in wildfire, including in the mesic forests of the Pacific Northwest where infrequent large high-severity fires resulted from warm-dry summers that enable fuel receptiveness and high winds that drive fire spread (Agee, 1996)—yet a systematic analysis of compound climate and weather factors in very large fires in western Oregon is lacking. Conceptual models of fire regimes consider the co-occurrence of biomass abundance, availability to burn, ignitions, and weather (Bradstock, 2010) and large wildfire events and seasons have been linked to compound drivers. For example, compound humidity and wind speed extremes are inherent features of many critical fire weather patterns (Crimmins, 2006), while the combination of critically dry fuels imparted by antecedent conditions combined with fire weather extremes have been connected with large fires and large fire seasons (e.g., Khorshidi et al., 2020; Williams et al., 2019). This study builds on previous efforts by applying different approaches for compound extremes that supported the growth of arguably the most exceptional fire outbreak in the Oregon Cascades in over a century.

In this study, we analyze the meteorological factors responsible for fire spread and antecedent climate factors that enabled fuel aridity of the wind-driven fires in the western Oregon Cascades whose explosive growth commenced on Labor Day 2020, hereafter referred to as the Labor Day fires. We first examine the synoptic and mesoscale meteorological conditions during the Labor Day fires and the rarity of individual meteorological and fuel aridity factors. We additionally use different approaches for quantifying the rarity of this event through the lens of compound extremes that combine fuel dryness and fire meteorology. Lastly, we systematically compare the compound climate and meteorological conditions during the Labor Day fires to other very large wildfire events in western Oregon since 1900.

2. Data and Methods

Meteorological and climatological data were obtained from several sources to address our research questions. First, we acquired hourly surface observations for operational automated surface observation stations (ASOS) and remote automated weather stations (RAWS) across Oregon from MesoWest (Horel et al., 2002) to examine patterns of near-surface wind and vapor pressure deficit (VPD) during the event. Second, 0Z wind speed and relative humidity observations at 1,000 hPa from version 2 of the Integrated Global Radiosonde Archive (Durre et al., 2006) for Salem, Oregon for the 64-year period 1957–2020 were used to contextualize meteorological conditions during the event against the longer-term data record. Third, daily 1/24th degree gridded meteorological data were acquired from gridMET (Abatzoglou, 2013) and used to calculate

two fire danger indices from the U.S. Fire Danger Rating System (Cohen & Deeming, 1985): Energy Release Component (ERC) and Burning Index (BI) for a commonly used fuel model (dense conifer) for 1979–2020. These data were used to contextualize fire danger during the event related to the past 42 years. Fourth, reanalysis products from the 20th Century Reanalysis v3 (Compo et al., 2011) during 1900–1947, NCEP-NCAR during 1948-present, and ERA5 (Hersbach et al., 2020) were used to examine mid-to-lower tropospheric synoptic conditions during the event, as well as to provide context relative to the longer-term record. Finally, gridded 1/24th degree monthly total precipitation and monthly mean daily maximum temperature for the period 1895–2020 were obtained from PRISM (Daly et al., 2008) for comparison of antecedent climate conditions during previous large fire events.

We use 700 and 850 hPa zonal wind velocity from reanalysis data as a simple and transparent indicator of cross-barrier downslope winds for the primarily north-south oriented Cascades rather than the more refined diagnostic approaches for downslope winds developed previously (Abatzoglou et al., 2020; Guzman-Morales et al., 2016). This was done by tabulating the maximum easterly wind velocity in the lower troposphere 700 or 850 hPa) near or just above the crest of the Oregon Cascades at 6-h intervals at two points: one in the Oregon Cascades at 45°N, 122.5°W, and the other in southwestern Oregon at 42.5°N, 122.5°W.

We accompany meteorological diagnostics with two fire danger indices—ERC and BI. ERC is proxy for fuel dryness and potential energy release at the front of a fire that is a function of antecedent temperature, precipitation, and humidity from previous several weeks and is independent of wind speed. ERC has been shown to influence large fire probability and interannual variability in regional area burned (Abatzoglou & Kolden, 2013; Barbero et al., 2014). BI combines ERC and potential rate of fire spread (chiefly a function of wind speed and fuel moisture) into a metric that is a proxy for flame length and fireline intensity. We examined statistics of BI as it provides a natural single metric of compound extremes of fuel moisture, atmospheric humidity, and wind speed that are of particular relevance for wind-driven fires.

We complement the assessment of compound extremes using rank/order statistics of interrelated drivers that allow for a more flexible treatment of the resultant hazard than functional equations built into a single index like BI. Two combinations were examined: (i) the joint distribution of 0Z relative humidity and wind speed at 1,000 hPa from Salem, Oregon radiosonde observations during 1957–2020; (ii) the joint distribution of ERC averaged for the Oregon Cascades ecoregion and lower-tropospheric easterly wind speed from reanalysis during 1979–2020. The former captures purely meteorological conditions, while the latter captures antecedent climate and meteorological conditions. Order/rank statistics have 1:1 accordance with probabilistic hazard assessment scenarios (Salvadori et al., 2016). While univariate order/rank statistics correspond directly to probability $P(X < x)$, multivariate order/rank statistics can take on several definitions. Herein, we follow previous studies that have used a bivariate case that corresponds to $P(X > x \text{ AND } Y > y)$. In this case, pairs are ranked as: $Z_i = [X_i, Y_i]$ dominates $Z_j = [X_j, Y_j]$, if X_i dominates X_j AND Y_i dominates Y_j (AghaKouchak et al., 2014; Alizadeh et al., 2020).

Lastly, we compiled a list of very large western Oregon wildfire events (35,000 ha) since 1900 (Table S1). We additionally included the 2017 Eagle Creek fire (19,761 ha) because it was the most recent large fire in the Oregon Cascades prior to 2020. Climate summaries for August, July–August, and June–August temperature and precipitation were aggregated from the counties in which each of large wildfire events occurred (Table S2). These periods were chosen because most of the very large fires ignited in August and/or September. For each fire event, we tabulated the maximum 6-h easterly wind during the estimated duration of the fire at 700 or 850 hPa from 20th Century Reanalysis and NCEP-NCAR for events prior to 1948 and those since 1948, respectively. We note there is some uncertainty about the extent and duration of the earliest fires, as well as potential omission of large fire events in the first-half of the 20th century due to poor documentation. The Labor Day fires of 2020 were contextualized with other very large fires within the trivariate space of antecedent temperature, antecedent precipitation, and concurrent easterly wind.

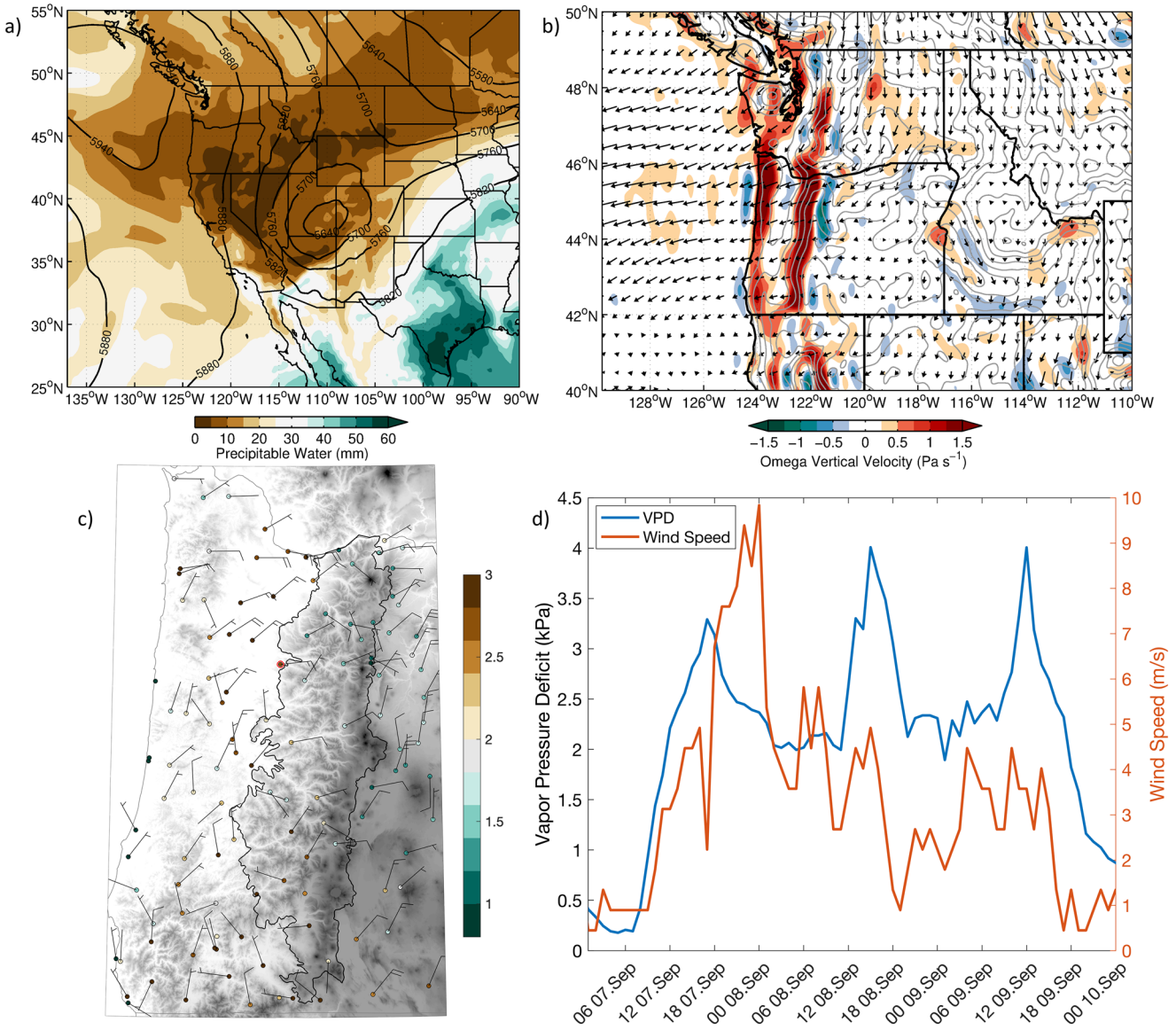

Figure 2. (a) Precipitable water (shading) and 500 hPa geopotential heights (contours, m), and (b) 850 hPa winds (vectors) and pressure vertical velocity (shading) at 0Z on 8 September 2020 (17 LST on 7 September). In (b), Gray contours show elevation, and red hues show downward motion while blue hues show upward motion. (c) Surface-based observations of wind speed (knots) and vapor pressure deficit (VPD, colors) at 20 LST on September 7, 2020. Gray shading in (c) depicts topography and black contour shows the Oregon Cascades ecoregion. (d) Time series of hourly wind speed and VPD from the Jordan RAWS station (red circle in panel c) during 7–9 September.

3. Results and Discussion

Critical fire weather conditions developed from eastern Washington state southward into western Oregon and northern California during September 7–8, 2020 resulting from an amplified wave across the Pacific-North American sector. An omega block off the coast of British Columbia and cut off low pressure near the U.S. four corners facilitated northeasterly flow and an intrusion of exceptionally dry air throughout much of the northwestern United States (Figure 2a). The onset of strong east-to-northeast (ENE) winds advanced from the northern portion of the Oregon Cascades during the afternoon of the seventh through southwestern Oregon into the morning of the eighth. Strong ENE cross-barrier lower-tropospheric winds developed across the Oregon Cascades exhibiting a classical signature of downslope winds and mountain lee wave evident by the wave pattern in ERA5 pressure vertical velocity fields and downward transport of strong easterly winds and dry air with relative humidities less than 10% in the lee of the Cascades (Figures 2a, 2b

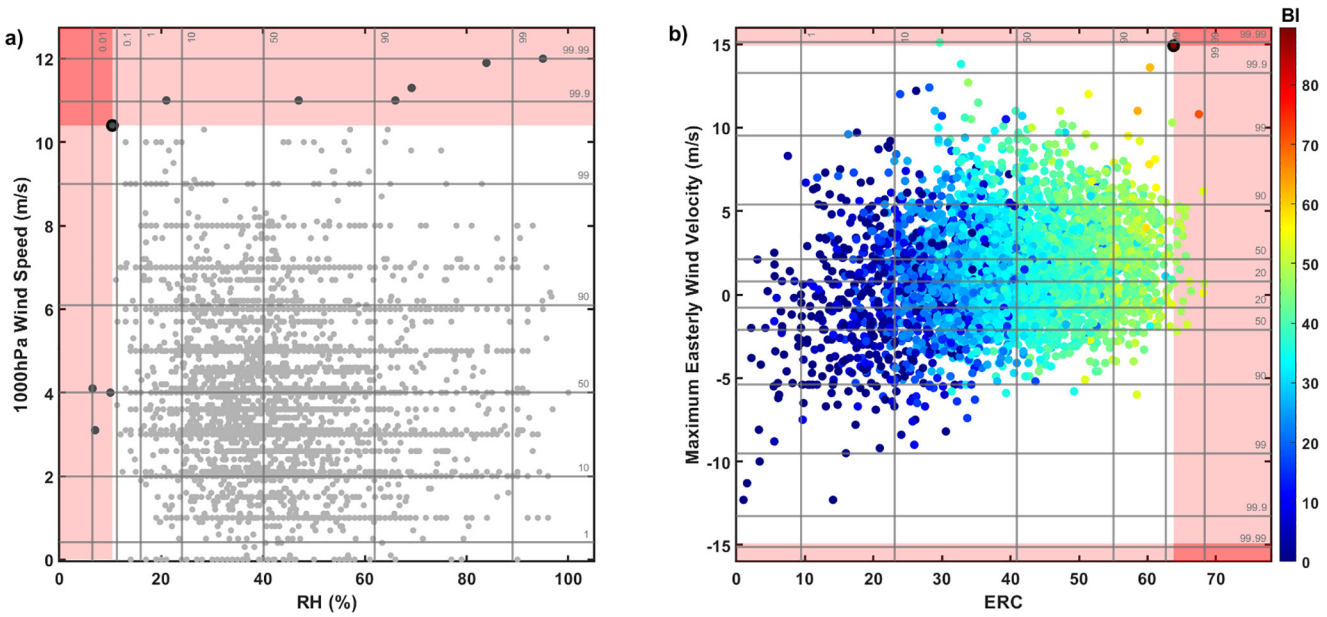

Figure 3. Scatter plots of (a) wind speed and relative humidity (RH) at 1000 hPa from the Salem, Oregon radiosonde for all July–September days during 1957–2020 at 0Z, and (b) daily maximum 6-h easterly wind velocity at 700/850 hPa from NCEP-NCAR reanalyzes and daily energy release component (ERC) averaged over the Oregon Cascades for all July–September days during 1979–2020. Negative easterly wind velocity refers to winds with a westerly component. Data in (b) are color-coded with daily burning index (BI) averaged over the Oregon Cascades. Points marked with black edge show data for 0Z September 9, 2020 (17 LST September 8, 2020) in (a) and 8 September 2020 in (b). Light-red shaded areas highlight the univariate space and events that exceed this point, while the dark-red shaded areas show the space that dominates this point in a bivariate AND-scenario case. Light gray horizontal and vertical lines show percentile values. Percentiles in both panels were computed relative to the entire July–September period of record. Percentiles are shown for wind speed in (b) rather than exclusively easterly wind velocity.

and S1). ERA5 precipitable water values were less than 10 mm over all of Oregon and upstream over much of the U.S. west (Figure 2a) on the afternoon of 7 September. The mesoscale manifestation of this pattern at 20 LST on September 7, 2020 shows widespread elevated surface VPD west of the Cascades and substantial heterogeneity in 10-m wind speeds imparted by topographic station siting (Figure 2c). The strongest low-level winds were primarily constrained to the evening of 7 and 8 September. Elevated VPD was seen for much of western Oregon for a sustained 2.5 day period starting the afternoon of the seventh and with little nocturnal recovery (Figure 2d).

Several individual meteorological elements of this event qualify as extremes. Observations of 1,000 hPa relative humidity and wind speed from the Salem sounding at 0Z 9 September (17 LST 8 September) were the fourth lowest and seventh highest values, respectively, for July–September in the 64-year period of record (Figure 3a). Importantly, extreme low RH conditions co-occurred with extreme high winds yielding the most extreme combination of dry-windy conditions for any July–September day during 1957–2020 when viewed through the bivariate lens (Figure 3a). Using the NCEP-NCAR reanalysis record from 1948–2020 and our diagnostic of offshore downslope winds, we find that September 8, 2020 had the second strongest easterly winds at 700 or 850 hPa for any July–September day (Figure S2).

Fire danger indices of ERC and BI remained near their 1981–2010 average values for much of July and early August across western Oregon (Figures 4c and 4d). However, for much of August and first week of September, unusually warm temperatures, elevated VPD, and negligible precipitation facilitated escalating fuel dryness and well above normal ERC in parts of western Oregon by early September (Figures 4a and 4c). On 8 September, both ERC and 700/850 hPa easterly wind speeds exceeded their respective 99th percentile values for July–September (Figure 3b). Similar to the meteorological drivers, the co-occurrence of extremely dry fuels and strong east winds resulted in a compound extreme unprecedented in the 42-year period of record, although none of the individual drivers were the most extreme. Complementary to rank/order statistics, we find widespread record BI across much of western Oregon on September 8, 2020 (Figure 4b) with 3 of the top 10 highest days of BI for the Oregon Cascades occurring during September 7–9, 2020 (Figure 4d). Hence,

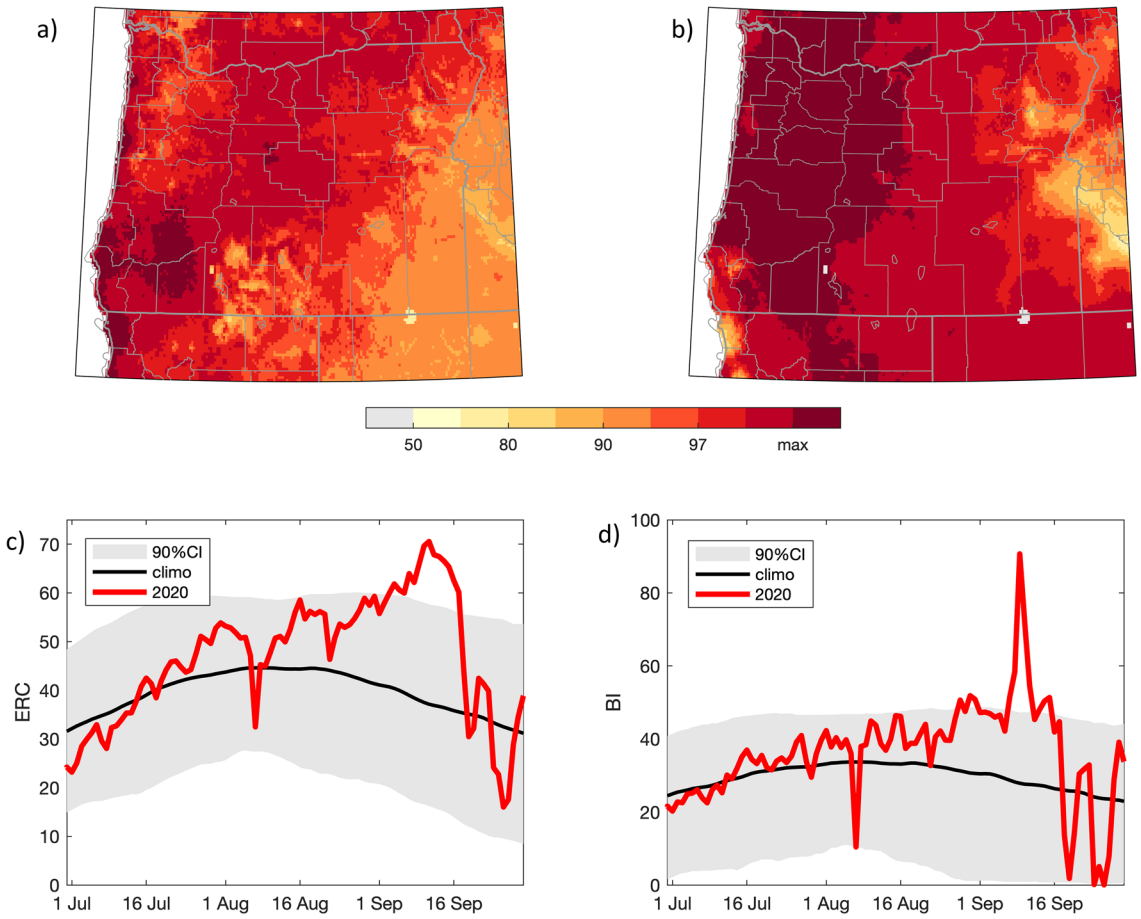

Figure 4. Percentiles of (a) Energy Release Component (ERC), and (b) Burning Index (BI) for September 8, 2020. Percentiles were tabulated based on data pooled over the entire calendar year 1979–2020. Time series of (c) ERC and (d) BI aggregated over the Oregon Cascades for 2020 (red), compared both the climatological 1981–2010 averages (black) and smoothed 5th to 95th percentile values (gray shading).

both approaches for quantifying compound extremes as a product of fuel dryness and potential rate of fire spread highlight conditions during the Labor Day fires as the most extreme in the observational record.

The majority (10 of 13) of very large fire events in western Oregon since 1900 were associated with a July–August that had below-median precipitation and above-median maximum temperatures (Figures 5, S3 and S4). Qualitatively similar results were found using June–August and August temperature and precipitation data, although with somewhat weaker results for precipitation (Figure S5). More recently, all seven very large fire events since 1987 had July–August precipitation at or below the 17th percentile and maximum temperature above the 70th percentile. Notably, July–August 2020 was neither the driest nor the warmest per these metrics.

All 13 very large fires were associated with a period of easterly lower-tropospheric wind during the fire event (Figure 5; see also Figure S6). The synoptic configuration corresponding to the days during each large fire event with the strongest easterly lower tropospheric flows showed similarity among previous events to the Labor Day fires (Figure S6) featuring a pronounced ridge off the coast, weak thermal trough along the Oregon coast, and northeastward gradient in mean sea level pressure across the region. No other very large fire had an easterly wind as strong as the 2020 Labor Day fires, nor were they associated with a 500-hPa level ridge and northeastward sea-level pressure gradient as strong. We note that potential inhomogeneities in reanalyzes products inhibited a robust comparison with fields such as wind velocity (Wohland et al., 2019; Figure S7). Notably, the 1902 Columbia fire had the second strongest easterly wind, yet the fire stands out by having neither a dry nor a warm July–August lead-up period (Figure 5), suggesting that it was more strongly a product of immediate meteorological conditions (Beals, 1914; Plummer, 1912). Previous

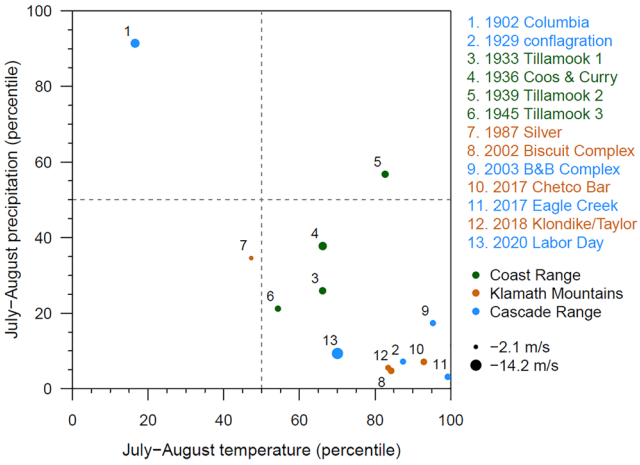

Figure 5. July–August total precipitation versus July–August mean daily maximum temperature for the years of the large wildfires in western Oregon listed in Table S1. Values are given as percentiles of the anomalies for the years 1895 through 2020 (126 years). The percentiles shown for each event are calculated with respect to the anomalies for the county/counties where the event occurred. Symbols are sized relative to the peak easterly wind component at 700 or 850 hPa at 45°N, 122.5°W from 6-hourly NCEP-NCAR reanalysis (1948-present) and 20th Century reanalysis (1900–1947).

studies have highlighted nonclimatic factors as contributors to large fires in the first half of the 20th century, primarily logging practices that increase dead fuel loading that help facilitate flammability in the absence of anomalously warm and dry summers (Dague, 1934; Kallander, 1953).

4. Conclusions

A series of factors contributed to the extent of fire impacts during the 2020 Labor Day fires in western Oregon that burned ~11% of the Oregon Cascades. A sequence of climate and weather factors enabled and drove rapid rates of fire spread following conceptual models of fire activity (Bradstock, 2010). Moreover, while individual factors such as humidity, wind speed, and fuel dryness were extreme, neither individually ranked as the most extreme on record. In contrast, compound extremes of fuel dryness and low-level wind speed, as well as wind speed and relative humidity, yielded conditions that were unprecedented in the contemporary data record. The extent of burned area across mesic forests of western Oregon during the 2020 Labor Day fires has no contemporary local analog. Very large fires (>200,000 ha) were documented in western Oregon in the 19th century coinciding with European colonization (Morris, 1934), although uncertainty of the location, timing, and contributing factors limit a more detailed comparison. The 2020 Labor Day fires do bear some resemblance to extremely large autumn wind-driven fires in California in terms of rapid rates of fire spread and materialization of compound extremes driven by offshore downslope winds at the end of the dry season when fuel moisture is critically low (Nauslar et al., 2018). Nonclimatic contributions to these fires imparted by biomass accumulation and land management practices (Reilly et al., 2017) also likely factored into this severity of fire impacts, although we do not speculate on their specific influences.

Very large fires with rapid rates of spread and extreme fire behavior are gaining attention as environmental phenomena that impact society and Earth system processes (Bowman et al., 2009; Khaykin et al., 2020). While the details of the meteorological, fuels, and topographic drivers of such extreme fires and their impacts vary (Tedim et al., 2018), requisite conditions of flammable contiguous fuels imparted by fuel drying enable extreme fires while meteorological conditions including strong winds or convection often drive rapid rates of fire spread (Bowman et al., 2017; Rothermel, 1991). Our findings of the Oregon 2020 Labor Day fires complement previous studies on compound drivers for autumn wind-driven fires in California (Khorshidi et al., 2020; Williams et al., 2019) and the development of fire early-warning systems (Jolly et al., 2019) while showing the potential use of the approach for individual fire events. Moreover, the approach used herein to quantify this extreme wind-driven fire events through the lens of compound extremes may have value in other regions with shared biophysical and human constraints on fire activity.

While unprecedent in the modern record, extreme events of this nature with widespread impact evoke questions on causality—namely the extent to which human-caused climate change contributed to the strength or probability of the event, as well as such events will become increasingly probable in the coming decades. A formal attribution exercise is beyond the scope of this analysis, yet studies suggest that climate change has contributed to increased fuel aridity and longer fire seasons (Abatzoglou & Williams, 2016) and the probability of compound hot-dry extremes (Alizadeh et al., 2020) and climate projections suggest continued warming with slight decreases in summer precipitation in the Pacific Northwest (Rupp et al., 2017) over the 21st century. By contrast, offshore winds such as Santa Ana winds in southern California may become less frequent as a result of asymmetric continental warming with anthropogenic forcing (Guzman-Morales & Gershunov, 2019; Hughes et al., 2011). However, few studies have formally evaluated these two contrasting drivers in a compound extremes framework (Goss et al., 2020). Projected changes in the confluence of extreme fire weather patterns and fuel dryness will be critical for resolving future fire related hazards for mesic forests in western Oregon and Washington state.

Data Availability Statement

Datasets used herein were acquired from the following public data repositories: (1) ERA5: https://cds.climate.copernicus.eu/; (2) NCEP-NCAR reanalysis: https://psl.noaa.gov/data/gridded/data.ncep.reanalysis.html; (3) twentieth Century Reanalysis v3: https://psl.noaa.gov/data/gridded/data.20thC_ReanV3.html; (4) gridMET: http://thredds.northwestknowledge.net:8080/thredds/reacch_climate_MET_catalog.html; (5) ASOS and RAWS station data: https://mesowest.utah.edu/; (6) PRISM data: https://prism.oregonstate.edu/.

Acknowledgments
J. T. Abatzoglou was supported by the NSF under award OAI-2019762 and NOAA awards NA15OAR4310145 and NA20OAR4310478. D. E. Rupp was supported by the NSF under award GEO 1740082. L. W. O'Neill was supported by the State of Oregon through the Oregon Climate Services.

References

Abatzoglou, J. T. (2013). Development of gridded surface meteorological data for ecological applications and modeling. *International Journal of Climatology*, *33*(1), 121–131. https://doi.org/10.1002/joc.3413

Abatzoglou, J. T., Hatchett, B. J., Fox-Hughes, P., Gershunov, A., & Nauslar, N. J. (2020). Global climatology of synoptically-forced downslope winds. *International Journal of Climatology*.

Abatzoglou, J. T., & Kolden, C. A. (2013). Relationships between climate and macroscale area burned in the western United States. *International Journal of Wildland Fire*, *22*(7), 1003–1020. https://doi.org/10.1071/wf13019

Abatzoglou, J. T., & Williams, A. P. (2016). Impact of anthropogenic climate change on wildfire across western US forests. *Proceedings of the National Academy of Sciences of the United States of America*, *113*(42), 11770–11775. https://doi.org/10.1073/pnas.1607171113

Agee, J. K. (1996). *Fire ecology of Pacific Northwest forests*. Island Press.

AghaKouchak, A., Cheng, L., Mazdiyasni, O., & Farahmand, A. (2014). Global warming and changes in risk of concurrent climate extremes: Insights from the 2014 California drought. *Geophysical Research Letters*, *41*(24), 8847–8852. https://doi.org/10.1002/2014gl062308

Alizadeh, M. R., Adamowski, J., Nikoo, M. R., AghaKouchak, A., Dennison, P., & Sadegh, M. (2020). A century of observations reveals increasing likelihood of continental-scale compound dry-hot extremes. *Science Advances*, *6*(39), eaaz4571. https://doi.org/10.1126/sciadv.aaz4571

Barbero, R., Abatzoglou, J. T., Steel, E. A., & Larkin, N. K. (2014). Modeling very large-fire occurrences over the continental United States from weather and climate forcing. *Environmental Research Letters*, *9*(12), 124009. https://doi.org/10.1088/1748-9326/9/12/124009

Beals, E. A. (1914). The value of weather forecasts in the problem of protecting forests from fire. *Monthly Weather Review*, *42*(2), 111–119. https://doi.org/10.1175/1520-0493(1914)42<111:tvowfi>2.0.co;2

Bowman, D. M. J. S., Balch, J. K., Artaxo, P., Bond, W. J., Carlson, J. M., Cochrane, M. A., et al. (2009). Fire in the Earth system. *Science*, *324*(5926), 481–484. https://doi.org/10.1126/science.1163886

Bowman, D. M. J. S., Williamson, G. J. G., Abatzoglou, J. T., Kolden, C. A., Cochrane, M. A., & Smith, A. M. S. (2017). Human exposure and sensitivity to globally extreme wildfire events. *Nature Ecology & Evolution*, *1*(3), 58. https://doi.org/10.1038/s41559-016-0058

Bradstock, R. A. (2010). A biogeographic model of fire regimes in Australia: Current and future implications. *Global Ecology and Biogeography*, *19*(2), 145–158. https://doi.org/10.1111/j.1466-8238.2009.00512.x

Cohen, J. E., & Deeming, J. D. (1985). *The National Fire-Danger Rating System: basic equations*. General Technical Report, 16.

Compo, G. P., Whitaker, J. S., Sardeshmukh, P. D., Matsui, N., Allan, R. J., Yin, X., et al. (2011). The twentieth century reanalysis project. *Quarterly Journal of the Royal Meteorological Society*, *137*(654), 1–28. https://doi.org/10.1002/qj.776

Cramer, O. P. (1957). *Frequency of dry east winds over northwest Oregon and southwest Washington*. Pacific Northwest Forest and Range Experiment Station: Forest Service.

Crimmins, M. A. (2006). Synoptic climatology of extreme fire-weather conditions across the southwest United States. *International Journal of Climatology*, *26*(8), 1001–1016. https://doi.org/10.1002/joc.1300

Dague, C. I. (1930). Disastrous fire weather of September, 1929. *Monthly Weather Review*, *58*, 368–370. https://doi.org/10.1175/1520-0493(1930)58<368:dfwos>2.0.co;2

Dague, C. I. (1934). The Weather of the Great Tillamook, Oreg., Fire of August 1933. *Monthly Weather Review*, *62*, 227–231. https://doi.org/10.1175/1520-0493(1934)62<227:twotgt>2.0.co;2

Daly, C., Halbleib, M., Smith, J. I., Gibson, W. P., Doggett, M. K., Taylor, G. H., et al. (2008). Physiographically sensitive mapping of climatological temperature and precipitation across the conterminous United States. *International Journal of Climatology*, *28*(15), 2031–2064. https://doi.org/10.1002/joc.1688

Durre, I., Vose, R. S., & Wuertz, D. B. (2006). Overview of the integrated global radiosonde archive. *Journal of Climate*, *19*(1), 53–68. https://doi.org/10.1175/jcli3594.1

Goss, M., Swain, D., Abatzoglou, J., Sarhadi, A., Kolden, C., Williams, A., & Diffenbaugh, N. (2020). Climate change is increasing the risk of extreme autumn wildfire conditions across California. *Environmental Research Letters*.

Guzman-Morales, J., & Gershunov, A. (2019). Climate change suppresses Santa Ana winds of southern California and sharpens their seasonality. *Geophysical Research Letters*.

Guzman-Morales, J., Gershunov, A., Theiss, J., Li, H., & Cayan, D. (2016). Santa Ana Winds of Southern California: Their climatology, extremes, and behavior spanning six and a half decades. *Geophysical Research Letters*, *43*(6), 2827–2834.

Hersbach, H., Bell, B., Berrisford, P., Hirahara, S., Horányi, A., Muñoz-Sabater, J., et al. (2020). The ERA5 global reanalysis. *Quarterly Journal of the Royal Meteorological Society*, *146*(730), 1999–2049. https://doi.org/10.1002/qj.3803

Higuera, P. E., & Abatzoglou, J. T. (2020). Record-setting climate enabled the extraordinary 2020 fire season in the western United States. *Global Change Biology*. https://doi.org/10.1111/gcb.15388

Horel, J., Splitt, M., Dunn, L., Pechmann, J., White, B., Ciliberti, C., et al. (2002). Mesowest: Cooperative mesonets in the western United States. *Bulletin of the American Meteorological Society*, *83*(2), 211–225. https://doi.org/10.1175/1520-0477(2002)083<0211:mcmitw>2.3.co;2

Hughes, M., Hall, A., & Kim, J. (2011). Human-induced changes in wind, temperature and relative humidity during Santa Ana events. *Climatic Change*, *109*(1), 119–132. https://doi.org/10.1007/s10584-011-0300-9

Jolly, W. M., Freeborn, P. H., Page, W. G., & Butler, B. W. (2019). Severe fire danger index: A forecastable metric to inform firefighter and community wildfire risk management. *Fire 2* 3 47. https://doi.org/10.3390/fire2030047

Kallander, R. M. (1953). *Problems of rehabilitating the Tillamook burn*. Retrieved from https://ir.library.oregonstate.edu/concern/graduate_thesis_or_dissertations/cj82kb40j

Khaykin, S., Legras, B., Bucci, S., Sellitto, P., Isaksen, L., Tencé, F., et al. (2020). The 2019/20 Australian wildfires generated a persistent smoke-charged vortex rising up to 35 km altitude. *Communications Earth & Environment*, *1*(1), 1–12. https://doi.org/10.1038/s43247-020-00022-5

Khorshidi, M. S., Dennison, P. E., Nikoo, M. R., AghaKouchak, A., Luce, C. H., & Sadegh, M. (2020). Increasing concurrence of wildfire drivers tripled megafire critical danger days in Southern California between 1982 and 2018. *Environmental Research Letters*, *15*(10), 104002. https://doi.org/10.1088/1748-9326/abae9e

Kolden, C., & Abatzoglou, J. (2018). Spatial distribution of wildfires ignited under katabatic versus non-katabatic winds in Mediterranean southern California USA. *Fire 1*(2), 19. https://doi.org/10.3390/fire1020019

Morris, W. G. (1934). Forest fires in western Oregon and western Washington. *Oregon Historical Quarterly*, *35*(4), 313–339.

Nauslar, N., Abatzoglou, J., & Marsh, P. (2018). The 2017 north Bay and southern California fires: A case study. *Fire*. https://doi.org/10.3390/fire1010018

Plummer, F. G. (1912). *Forest fires: Their causes, extent, and effects, with a summary of recorded destruction and loss*. US Department of Agriculture, Forest Service.

Reilly, M. J., Dunn, C. J., Meigs, G. W., Spies, T. A., Kennedy, R. E., Bailey, J. D., & Briggs, K. (2017). Contemporary patterns of fire extent and severity in forests of the Pacific Northwest, USA (1985–2010). *Ecosphere*, *8*(3), e01695. https://doi.org/10.1002/ecs2.1695

Rothermel, R. C. (1972). A mathematical model for predicting fire spread in wildland fuels. Intermountain Forest & Range Experiment Station, Forest Service.

Rothermel, R. C. (1991). Predicting behavior and size of crown fires in the northern rocky mountains. US Department of Agriculture, Forest Service, Intermountain Forest and Range.

Rupp, D. E., Li, S., Mote, P. W., Shell, K. M., Massey, N., Sparrow, S. N., et al. (2017). Seasonal spatial patterns of projected anthropogenic warming in complex terrain: A modeling study of the western US. *Climate Dynamics*, *48*(7–8), 2191–2213. https://doi.org/10.1007/s00382-016-3200-x

Sadegh, M., Moftakhari, H., Gupta, H. V., Ragno, E., Mazdiyasni, O., Sanders, B., et al. (2018). Multihazard scenarios for analysis of compound extreme events. *Geophysical Research Letters*, *45*(11), 5470–5480. https://doi.org/10.1029/2018gl077317

Salvadori, G., Durante, F., De Michele, C., Bernardi, M., & Petrella, L. (2016). A multivariate copula-based framework for dealing with hazard scenarios and failure probabilities. *Water Resources Research*, *52*(5), 3701–3721. https://doi.org/10.1002/2015wr017225

Seneviratne, S., Nicholls, N., Easterling, D., Goodess, C., Kanae, S., Kossin, J., et al. (2012). *Changes in climate extremes and their impacts on the natural physical environment*. In: IPCC WGI/WGII Special Report on Managing the Risks of Extreme Events and Disasters to Advance Climate Change Adaptation (SREX), (pp. 109–230). Cambridge England.

Sharples, J. J., Mills, G. A., McRae, R. H. D., & Weber, R. O. (2010). Foehn-like winds and elevated fire danger conditions in southeastern Australia. *Journal of Applied Meteorology and Climatology*, *49*(6), 1067–1095. https://doi.org/10.1175/2010jamc2219.1

State of Oregon. (2021). Retrieved from https://www.oregon.gov/gov/policy/Documents/WERC-2020/Wildfire%20Report%20FINAL.pdf

Tedim, F., Leone, V., Amraoui, M., Bouillon, C., Coughlan, R. M., Delogu, M. G., et al. (2018). Defining extreme wildfire events: Difficulties, challenges, and impacts. *Fire*. https://doi.org/10.3390/fire1010009

Williams, A. P., Abatzoglou, J. T., Gershunov, A., Guzman-Morales, J., Bishop, D. A., Balch, J. K., & Lettenmaier, D. P. (2019). Observed impacts of anthropogenic climate change on wildfire in California. *Earth's Future*, *7*, 892–910. https://doi.org/10.1029/2019ef001210

Wohland, J., Omrani, N. E., Witthaut, D., & Keenlyside, N. S. (2019). Inconsistent wind speed trends in current twentieth century reanalyzes. *Journal of Geophysical Research - D: Atmospheres*, *124*(4), 1931–1940. https://doi.org/10.1029/2018jd030083